

# A NUMERICAL METHOD FOR DISCRETE ORDINATE AND MOMENT EQUATIONS IN RADIATIVE TRANSFER†

PHILIP M. CAMPBELL

Department of Physics and Astronomy, The University of New Mexico, Albuquerque, New Mexico 87106

(Received 20 March 1968 and in revised form 30 August 1968)

**Abstract**—A method is presented for the numerical solution of nonlinear, frequency-dependent radiative transfer problems with one-dimensional symmetry. The principal feature of the method is accuracy of the finite difference scheme in the limits of large and small cross sections. The method is illustrated in a number of sample calculations.

## NOMENCLATURE

$a$ ,	radiation constant $8\pi^5 k^4/15c^3 h^3$ ;	$K_l$ ,	coefficients in Legendre polynomial expansion of $K(\mu, \mu')$ ;
$A_b$ ,	quadrature coefficient for integrals over angle;	$L_k^N(\mu)$ ,	coefficients in the Lagrange interpolating polynomial;
$A'_k$ ,	quadrature coefficient for integrals over frequency;	$M_k^y(r, t)$ ,	moments of the angular distribution;
$c$ ,	velocity of light;	$N$ ,	order of approximation in angular representations;
$c_v$ ,	specific heat at constant volume;	$P^y(r, t)$ ,	$r$ component of radiation pressure tensor;
$C_l^N$ ,	coefficients of Legendre polynomial of order $N$ ;	$P_l(\mu)$ ,	Legendre polynomial of order $l$ ;
$D_{l, k}$ ,	coefficients of angular derivative;	$r$ ,	position coordinate;
$E_m(T)$ ,	material energy density;	$S_l^y$ ,	scattering term in discrete ordinate equations;
$E^y(r, t)$ ,	radiation energy density;	$t$ ,	time;
$F^y(r, t)$ ,	$r$ component of energy flux density;	$T$ ,	temperature;
$E, F$ ,	corresponding frequency-integrated quantities;	$T^*$ ,	first approximation to $T^{n+\frac{1}{2}}$ .
$h$ ,	Planck's constant;		
$I^y(r, \mu, t)$ ,	monochromatic specific intensity of radiation;		
$I_j^n(l, k)$ ,	corresponding difference form;		
$I(r, \mu, t)$ ,	frequency integrated intensity;		
$i$ ,	$\sqrt{-1}$ ;		
$k$ ,	Boltzmann constant (when used with $T$ );		
$k_{\max}$ ,	maximum number of frequency intervals;		
$K(\mu, \mu')$ ,	scattering kernel averaged over azimuth angle;		

## Greek symbols

$\alpha$ ,	geometry index;
$\Delta r$ ,	small increment in position;
$\Delta t$ ,	time increment;
$\Delta V_j$ ,	volume of zone $j$ ;
$\lambda$ ,	mean free path;
$\bar{\lambda}_R$ ,	Rosseland mean free path;
$\mu$ ,	direction cosine relative to $r$ axis;
$\mu_i$ ,	points of division in the $\mu$ interval;
$\nu$ ,	frequency of radiation;
$\rho$ ,	mass density;
$\sigma_a^y$ ,	absorption cross section in units of $(\text{length})^{-1}$ ;

† This work performed under the auspices of the U.S. Atomic Energy Commission.

$\sigma_s$ ,	scattering cross section;
$\bar{\sigma}_p$ ,	Planck mean absorption cross section;
$\psi_l^j(r, t)$ ,	coefficients in Legendre polynomial expansion of intensity.
Subscripts	
0,	indicates a given reference value which is constant;
$j$ ,	refers to the space mesh position $r_j = j \Delta r$ ;
$j + \frac{1}{2}$ ,	refers to the center of zone $j$ ;
$k, l$ ,	general summation indices in section 4;
$k$ ,	a frequency index in any difference equation;
$l$ ,	an angular index in any difference equation.
Superscripts	
$v$ ,	frequency index;
$n$ ,	refers to time $t^n = n \Delta t$ .

## 1. INTRODUCTION

THIS paper is concerned with a method for numerical computation of the radiative heating and cooling of material objects. The method is designed for problems in which the full transport equation is required [1]. These problems usually involve high temperatures or low densities, such as those encountered in nuclear explosions or the re-entry of space vehicles into the atmosphere.

A radiation field at any point is composed of components with different frequencies and consequently a wide range of absorption mean free path. The usual finite difference procedures for the transport equation [2, 3] are only accurate for space and time differences small compared to the mean free path. These methods are therefore too restrictive to use in most frequency-dependent calculations.

In order to solve a frequency-dependent problem efficiently, a single method is needed that is accurate for a wide range of cross sections. One method of this type is based on

Monte Carlo techniques [4]. In the present paper, a finite difference method is developed that is accurate regardless of the size of the cross sections. This method is superior to the Monte Carlo in terms of accuracy and computer time for most problems with simple geometry.

In section 2 a statement of the problem is given, and the general procedure for solving the basic equations is discussed. In section 3 the cross sections and the differencing of the frequency spectrum are described.

In section 4 the discrete ordinate and moment representations of the angular distribution are given. These angular representations have been shown to be equivalent.

In section 5 a numerical method for the moment equations is developed that is accurate for both large and small cross sections. An equivalent method for the discrete ordinate equations is given in section 6. The method is demonstrated with the solution of representative problems in section 7.

## 2. BASIC EQUATIONS

In the linear problem of radiative transfer, the emitting and absorbing properties of the material are given. In the nonlinear problem, these properties depend on the temperature and must be determined as part of the calculation. In this section the basic equations for the nonlinear problem are given in both plane and spherical geometry, assuming local thermodynamic equilibrium and conservative scattering.

The transport equation is

$$\frac{1}{c} \frac{\partial I^v}{\partial t} + \mu \frac{\partial I^v}{\partial r} + \frac{\alpha(1 - \mu^2)}{2r} \frac{\partial I}{\partial \mu} + (\sigma_a^v + \sigma_s) I^v = \bar{\sigma}_a^v B^v(T) + \sigma_s \int_{-1}^1 K(\mu, \mu') I^v(\mu') d\mu', \quad (2.1)$$

where  $\alpha = 0$  for plane geometry and  $\alpha = 2$  for spherical geometry. The temperature at any point in the material depends on the history of energy exchange with the radiation field. When

equation (2.1) is multiplied by  $2\pi$  and integrated over all  $\mu$  and  $\nu$ , the equation of energy conservation is obtained

$$\frac{\partial E}{\partial t} + \frac{1}{r^2} \frac{\partial}{\partial r} (r^2 F) = \int_0^\infty c \sigma_a^\nu \left[ \frac{4\pi}{c} B^\nu(T) - E^\nu \right] d\nu$$

$$= - \frac{\partial}{\partial t} E_m(T). \quad (2.2)$$

In equation (2.2),  $E$  and  $F$  are the radiation energy and energy flux densities, and  $E_m(T)$  is the thermal energy density in the material. The material energy density must be given as a function of temperature by the equation of state,

$$E_m(T) = \rho c_v T. \quad (2.3)$$

In general the specific heat  $c_v$  will depend on the temperature, but for the purposes of this paper it will be assumed constant.

The nonlinear problem is described by the following set of basic equations: The transport equation (2.1) with the appropriate boundary conditions, the energy balance equations (2.2), the equation of state (2.3), and expressions for the cross sections and scattering kernel.

In order to solve this set of coupled integro-differential equations, they will be approximated by a set of finite difference equations [5, 6] on a net of points covering the region in which the solution is required. There are no generally accepted rules by which to obtain the best difference equations for a numerical calculation. However, the following principle is a valuable guide:

*The most important properties of the basic equations should be built into the differencing scheme so that these properties are automatically present in the lowest order of approximation.*

The principle insures that the critical features of the basic equations are realized with any net spacing, and not just in the limit as the net spacing approaches zero. One such feature is energy conservation. In a nonlinear calculation

where the equations of transport (2.1) and energy balance (2.2) are used together, their difference forms must be consistent. Another desirable feature is accuracy of the difference equations regardless of the size of the net spacing relative to the mean free path.

### 3. FREQUENCY SPECTRUM

Since the frequency appears only as a parameter in equation (2.1), the frequency distribution of  $I(r, \mu, t)$  can be differenced independently of the other variables. This differencing will be determined by the form of the cross sections. Actual cross sections that include lines and absorption edges are quite complicated [7]. Such cases will be avoided here in order to concentrate on the problems of space-time and angular differencing.

For the purpose of illustrating the numerical method, an absorption cross section of the form

$$\sigma_a^\nu = \sigma_0 \left( \frac{h\nu}{kT_0} \right)^{-3} [1 - \exp(-h\nu/kT)] \quad (3.1)$$

is assumed, where the exponential term corrects for induced emission. The Thompson scattering kernel,

$$K(\mu, \mu') = \frac{3}{16} [(3 - \mu^2) + (3\mu^2 - 1)\mu'^2], \quad (3.2)$$

will be used with  $\sigma_s = \text{const}$ .

Since the cross sections are simple, a uniform division of the frequency interval can be used,

$$\nu_k = k\Delta\nu \quad k = 0, 1, \dots, k_{\max}$$

where  $k_{\max}$  is chosen large enough so that the radiant energy in all higher frequencies is negligible. Integrals over frequency are then obtained by

$$I(r_j, \mu_l, t^n) = \sum_{k=0}^{k_{\max}} A'_k I_j^n(l, k),$$

where  $A'_k$  are the quadrature coefficients for Simpson's rule, and  $k_{\max}$  is an even integer.

#### 4. MOMENT AND DISCRETE ORDINATE REPRESENTATIONS

The angular distribution of the radiation field can be expressed approximately in three different representations: Legendre polynomial, angular moment, and discrete ordinate. The equivalence of these representations has been discussed in restricted cases by several authors. In Chapter 7 of Richtmyer [6], the equivalence between the discrete ordinate and Legendre polynomial equations is demonstrated for neutron transport in plane geometry. Chandrasekhar [8] states that his version of discrete ordinates in spherical geometry is equivalent to the Legendre polynomial equations. Krook [9] has demonstrated the equivalence of all three representations for the Milne problem, i.e. steady state radiative transfer in plane geometry with isotropic scattering.

The equivalence of the three angular representations can also be shown for the nonlinear problem of radiative transfer with Thompson scattering in plane and spherical geometry. In the remainder of this section, the basic equations for radiative transfer in the moment and discrete ordinate representations are given, and in the following sections a finite difference method for the solution of these equations is developed. The difference scheme for the discrete ordinate equations is based on the equivalence between the angular representations.

##### (a) Angular moment representation

In this representation the angular distribution of the radiation field is expressed in terms of its moments:

$$M_k^y(r, t) = 2\pi \int_{-1}^1 I^y(r, \mu, t) \mu^k d\mu,$$

$$k = 0, 1, 2, \dots$$

The moments determine the coefficients in a Taylor series expansion of the Fourier transform of  $I^y(r, \mu, t)$  [10].

When the transport equation (2.1) is multi-

plied by  $2\pi\mu^k d\mu$  and integrated, the following sequence of moment equations is obtained:

$$\begin{aligned} \frac{1}{c} \frac{\partial M_k^y}{\partial t} + \frac{\partial M_{k+1}^y}{\partial r} + \frac{\alpha}{2r} \left[ (k+2) M_{k+1}^y - k M_{k-1}^y \right] \\ + (\sigma_a^y + \sigma_s) M_k^y = 2\pi \frac{[1 + (-1)^k]}{(k+1)} \sigma_a^y B^y(T) \\ + 2\pi \sigma_s G_k^y, \quad k = 0, 1, 2, \dots \end{aligned} \quad (4.1)$$

where  $G_k^y$  is the scattering term. In any  $N-1$  moment equations there are  $N$  unknowns. If the sequence is truncated by the relation

$$\sum_{k=0}^N C_k^N M_k^y = 0, \quad (4.2)$$

where the  $C_k^N$  are coefficients of the Legendre polynomial

$$P_N(\mu) = \sum_{k=0}^N C_k^N \mu^k,$$

the moment representation will be equivalent to the Legendre polynomial representation.

##### (b) Discrete ordinate representation

In this representation, the  $\mu$  interval  $(-1, 1)$  is subdivided by  $N$  points  $\mu_i$ , where the points of division are the zeros of  $P_N(\mu)$ . The angular distribution is then given by a Lagrange interpolating function

$$I^y(r, \mu, t) = \sum_{k=1}^N L_k^N(\mu) I_k^y(r, t), \quad (4.3)$$

where  $I_k^y(r, t)$  are the discrete ordinates, and the Lagrangian coefficients [11] are

$$L_k^N(\mu) = \frac{P_N(\mu)}{(\mu - \mu_k)} \left[ \frac{dP_N}{d\mu} \right]_{\mu=\mu_k}^{-1}$$

When the angular distribution is given by (4.3), the angular derivatives at each of the points of division are

$$\left[ \frac{\partial I}{\partial \mu} \right]_{\mu_i} = \sum_{k=1}^N I_k^y \left[ \frac{dL_k(\mu)}{d\mu} \right]_{\mu=\mu_i} \equiv \sum_{k=1}^N D_{i,k} I_k^y, \quad (4.4)$$

and the integral of the intensity is given by the Gaussian quadrature formula

$$\int_{-1}^1 I^\nu d\mu = \sum_{k=1}^N I_l^\nu \int_{-1}^1 L_l(\mu) d\mu \equiv \sum_{k=1}^N A_l I_l^\nu. \quad (4.5)$$

The transport equation (2.1) for discrete ordinates becomes

$$\begin{aligned} \frac{1}{c} \frac{\partial I_l^\nu}{\partial t} = \mu_l \frac{\partial I_l^\nu}{\partial r} + \frac{\alpha(1-\mu_l^2)}{2r} \sum_k D_{l,k} I_k^\nu \\ + (\sigma_a^\nu + \sigma_s) I_l^\nu = \sigma_a^\nu B^\nu(T) + \sigma_s S_l^\nu, \\ l = 1, 2, \dots, N \end{aligned} \quad (4.6)$$

where  $S_l^\nu$  is the scattering term.

In this representation, the angular moments are given in terms of the discrete ordinates by

$$M_k^\nu = 2\pi \sum_{l=1}^N I_l^\nu \int_{-1}^1 L_l(\mu) \mu^k d\mu, \quad k = 0, 1, 2, \dots, N.$$

When the Lagrange coefficients  $L_l(\mu)$  are expressed in terms of  $P_N(\mu)$ , the integral can be evaluated using the orthogonality property of the Legendre functions. The result is

$$M_k^\nu = 2\pi \sum_{l=1}^N A_l I_l^\nu \mu_l^k, \quad k = 0, 1, 2, \dots, N \quad (4.7)$$

where the  $A_l$  are the quadrature coefficients defined by (4.5). It should be emphasized that only for Gaussian quadrature are the moments given in terms of the discrete ordinates by (4.7).

The expression (4.7) is fundamental to the equivalence of the difference schemes discussed in the two following sections.

### 5. MOMENT EQUATIONS FOR LARGE AND SMALL CROSS SECTIONS

The equations of the moment representation (4.1) are particularly well suited for transport calculations in the limits of large and small cross sections. These equations allow several levels of approximation that are not obtained in the usual treatment [1] of transport in

optically thick and thin materials. When expressed in terms of energy density, flux density, and radiation pressure, the first two moment equations become

$$\frac{\partial E^\nu}{\partial t} + \frac{1}{r^\alpha} \frac{\partial}{\partial r} (r^\alpha F^\nu) + c\sigma_a^\nu E^\nu = 4\pi\sigma_a^\nu B^\nu(T) \quad (5.1a)$$

$$\begin{aligned} \frac{1}{c} \frac{\partial F^\nu}{\partial t} + c \frac{\partial P^\nu}{\partial r} + \frac{\alpha c}{2r} (3P^\nu - E^\nu) \\ + (\sigma_a^\nu + \sigma_s) F^\nu = 0, \end{aligned} \quad (5.1b)$$

where the energy balance equation is

$$\frac{\partial}{\partial t} E_m(T) = \int_0^\infty c\sigma_a^\nu \left[ E^\nu - \frac{4\pi}{c} B^\nu(T) \right] d\nu. \quad (5.1c)$$

In the two approximations to be considered,  $P^\nu$  is determined by the geometry of the problem, and no higher moments need to be included.

For those frequencies with very small cross section,

$$\left| \frac{1}{c} \frac{\partial F^\nu}{\partial t} \right| \gg \left| \sigma_a^\nu F^\nu \right|$$

and in most problems  $\sigma_s \ll \sigma_a^\nu$ . The last term in (5.1b) can therefore be neglected. The third term does not appear in plane geometry, and in spherical geometry it will be much smaller than the second term, except perhaps near the center.

If the cross sections are small, the radiation field will be dominated by the external sources rather than by local emission from the material. Under these conditions, the radiation pressure is given by  $P^\nu \simeq E^\nu$  (the relation for a plane or spherical wave), and the transport problem is described by the *free wave* approximation:

$$\frac{\partial E^\nu}{\partial t} + \frac{1}{r^\alpha} \frac{\partial}{\partial r} (r^\alpha F^\nu) + c\sigma_a^\nu E^\nu = 4\pi\sigma_a^\nu B^\nu(T), \quad (5.2a)$$

$$\frac{1}{c} \frac{\partial F^\nu}{\partial t} + c \frac{\partial E^\nu}{\partial r} \simeq 0. \quad (5.2b)$$

Note that when  $\sigma_a^v = \sigma_s = 0$ , the equations (5.2) reduce to the equations of wave propagation with velocity  $c$  in either plane or spherical geometry.

For frequencies with moderately large cross section,

$$\left| \frac{1}{c} \frac{\partial F^v}{\partial t} \right| \ll \left| \sigma_a^v F^v \right|,$$

and the local isotropic emission from the material will dominate the radiation field. For isotropic radiation  $P^v = E^v/3$ , and (5.1b) reduces to the relation for flux in a diffusing medium. The transport problem is then described by the *nonequilibrium diffusion* approximation:

$$\frac{\partial E^v}{\partial t} + \frac{1}{r^2} \frac{\partial}{\partial r} (r^2 F^v) + c \sigma_a^v E^v = 4\pi \sigma_a^v B^v(T), \quad (5.3a)$$

$$F^v \cong -\frac{c}{3} (\sigma_a^v + \sigma_s)^{-1} \frac{\partial E^v}{\partial r}. \quad (5.3b)$$

When the cross section is exceedingly large for all frequencies, the temperature distribution rapidly comes into equilibrium with the radiation field so that  $E^v \simeq (4\pi/c) B^v(T)$  everywhere. In this case the frequency spectrum is determined, thereby permitting the use of frequency-integrated equations in the *equilibrium diffusion* approximation:

$$E = aT^4, F = -\frac{c}{3} \bar{\lambda}_R \frac{\partial E}{\partial r} \quad (5.4a)$$

$$\frac{\partial E_m}{\partial t} + \frac{\partial E}{\partial t} + \frac{1}{r^2} \frac{\partial}{\partial r} (r^2 F) = 0, \quad (5.4b)$$

where the Rosseland mean free path is defined by

$$\bar{\lambda}_R \equiv \left[ \int_0^\infty (\sigma_a^v + \sigma_s)^{-1} \frac{\partial B^v}{\partial T} dv \right] \left[ \int_0^\infty \frac{\partial B^v}{\partial T} dv \right]^{-1}.$$

Note that both the free wave approximation and the nonequilibrium diffusion approximation are contained in the first two moment

equations, provided that  $P^v$  is given. These two equations, therefore, hold most of the content of the transport process. The moment equations of all higher orders merely serve to determine  $P^v$ . In most cases  $P^v$  is approximated very well by  $P^v = \beta E^v$ , where the Eddington factor  $\beta$  usually falls in the range  $\frac{1}{3} \leq \beta \leq 1$ .

In constructing difference equations for (5.1), one must be careful to insure that the correct difference forms for the diffusion equation and wave equation result in the limits of large and small cross section. By the guiding principle adopted in section 2, this property must be directly built into the difference form of (5.1). A difference form of this kind is obtained if the energy density  $E_{j+\frac{1}{2}}^n$  and temperature  $T_{j+\frac{1}{2}}^n$  are defined at zone centers, and the flux  $F_j^n$  is defined at zone boundaries as in Fig. 1. The difference form of (5.1) then becomes

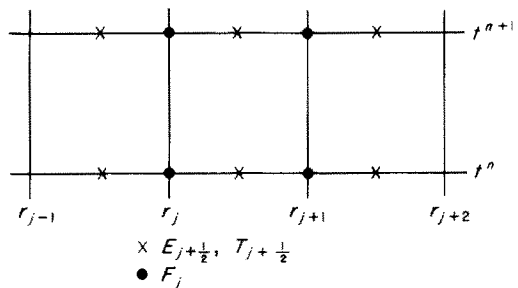


FIG. 1. A section of the space-time difference net, showing the points of definition for temperature, energy density, and energy flux density.

$$\frac{E_{j+\frac{1}{2}}^{n+1} - E_{j+\frac{1}{2}}^n}{\Delta t} - \frac{(r^2 F)_{j+\frac{1}{2}}^{n+1} - (r^2 F)_{j+\frac{1}{2}}^n}{r_{j+\frac{1}{2}}^2 \Delta r} + c \sigma_a^v \frac{1}{2} (E_{j+\frac{1}{2}}^{n+1} + E_{j+\frac{1}{2}}^n) = 4\pi \sigma_a^v B^v(T_{j+\frac{1}{2}}^{n+\frac{1}{2}}), \quad (5.5a)$$

$$\frac{F_j^{n+1} - F_j^n}{c \Delta t} + c \frac{P_{j+\frac{1}{2}}^{n+\frac{1}{2}} - P_{j-\frac{1}{2}}^{n+\frac{1}{2}}}{\frac{1}{2}(r_{j+1} - r_{j-1})} + \frac{\alpha c}{2r_j} (3P_j^{n+\frac{1}{2}} - E_j^{n+\frac{1}{2}}) + (\sigma_a^v + \sigma_s) \frac{1}{2} (F_j^{n+1} + F_j^n) = 0. \quad (5.5b)$$

In (5.5) the frequency index is suppressed for

convenience in notation, and any quantity defined at  $t^{n+\frac{1}{2}}$  is given by  $T^{n+\frac{1}{2}} = \frac{1}{2}(T^{n+1} + T^n)$ .

Inspection of (5.5) shows that when the cross sections are large and  $P^v \simeq E^v/3$ , these equations reduce to the Crank-Nicholson difference form [12] of the diffusion equation. When the cross sections are small and  $P^v \simeq E^v$ , the equations (5.5) reduce to the corresponding difference form of the wave equation [13].

The first two equations (5.1a) and (5.1b) are fundamental to any calculation based on moments. There are several alternate ways of obtaining the second moment  $P^v$ . One can consider any number of higher moment equations, differenced as in (5.5), with an appropriate truncation formula; one can use for the second moment equation

$$\frac{1}{c} \frac{\partial F^v}{\partial t} + c \frac{\partial E^v}{\partial r} + 3(\mathcal{J}_a^v + \sigma_s) F^v = 0,$$

a form [14] which automatically gives the two asymptotic expressions (5.2b) and (5.3b); or one can calculate the Eddington factor  $\beta$  approximately for different configurations on the basis of known analytic solutions [15].

The three approximations (5.2), (5.3), and (5.4) have been compared by Campbell and Nelson [16] with Monte Carlo transport solutions [4] for small, intermediate, and large cross sections. The expected accuracy of these approximations is confirmed.

## 6. DISCRETE ORDINATE METHOD FOR COMBINED TRANSPORT AND RADIATION DIFFUSION

In section 5 a difference method for the moment equations was given that automatically insures the correct transport properties for both large and small cross sections. Since the discrete ordinate and moment representations are consistent and equivalent in accuracy, it should be possible to find a space-time difference scheme for the discrete ordinate equations equivalent to (5.5). Such a difference scheme is presented here. It gives  $P^v$  to sufficient accuracy and also reduces to the diffusion and wave approxima-

tions for large and small cross sections. In the interests of simplicity, the method is described for plane geometry only.

The specific intensity is denoted by

$$I^v(r_j, \mu_l, t^n) \equiv I_j^n(l, k),$$

although some of the indices may not be written out explicitly. The calculation requires two sets of intensities, one set defined at the zone boundaries,  $I_j^n$ , and the other at zone centers,  $I_{j+\frac{1}{2}}^n$ . The temperatures and mass densities are zone-centered. At each time step, all the quantities are given at  $t^n$  and  $t^{n-1}$ , and the calculation proceeds as follows:

### (a) Predicted intensities

In order to start the calculation, provisional values of the intensity and temperature are needed at  $t^{n+1}$ . These quantities are obtained by linear extrapolation.

### (b) Calculation of zone boundary intensities

The zone boundary intensities at  $t^{n+1}$  are calculated from the following difference form of (4.6):

$$\begin{aligned} \frac{I_j^{n+1} - I_j^n}{c\Delta t} + \mu_l \frac{I_{j+\frac{1}{2}}^{n+1} + I_{j+\frac{1}{2}}^n - I_{j-\frac{1}{2}}^{n+1} - I_{j-\frac{1}{2}}^n}{(r_{j+1} - r_{j-1})} \\ + (\sigma_a^v + \sigma_s) \frac{1}{2}(I_j^{n+1} + I_j^n) \\ = \sigma_a^v B^v(T_j^{n+\frac{1}{2}}) + \sigma_s S_j^{n+\frac{1}{2}}, \end{aligned} \quad (6.1)$$

where

$$T_j^{n+\frac{1}{2}} = \frac{1}{4}(T_{j+\frac{1}{2}}^{n+1} + T_{j+\frac{1}{2}}^n + T_{j-\frac{1}{2}}^{n+1} + T_{j-\frac{1}{2}}^n),$$

and the scattering term is evaluated in terms of *predicted intensities*,

$$S_j^{n+\frac{1}{2}} = \sum_l \frac{1}{2} [I_j^{n+1}(l, k) + I_j^n(l, k)] A_l K(\mu_l, \mu_l).$$

When the corrected intensities  $I_j^{n+1}$  are obtained from (6.1), the zone boundary fluxes are determined by the quadrature formula

$$F_j^{n+\frac{1}{2}}(v_k) = 2\pi \sum_l A_l \mu_{l2}^{\frac{1}{2}} [I_j^{n+1}(l, k) + I_j^n(l, k)]. \quad (6.2)$$

The form of (6.1) is such that the fluxes obey (5.5b) by virtue of (4.7).

(c) *Calculation of temperatures*

Knowledge of the boundary fluxes now permits the calculation of zone temperatures. The energy densities in each frequency group are obtained from

$$\frac{E_{j+\frac{1}{2}}^{n+1} - E_{j+\frac{1}{2}}^n}{\Delta t} + \frac{F_{j+\frac{1}{2}}^{n+1} - F_{j+\frac{1}{2}}^n}{r_{j+1} - r_j} + c\sigma_a^{v_k} \frac{1}{2}(E_{j+\frac{1}{2}}^{n+1} + E_{j+\frac{1}{2}}^n) = 4\pi\sigma_a^{v_k} B^{v_k}(T_{j+\frac{1}{2}}^*), \quad (6.3)$$

together with the Planck mean,

$$\bar{\sigma}_p(T_{j+\frac{1}{2}}^*) = \frac{4\pi}{ac} (T_{j+\frac{1}{2}}^*)^{-4} \sum_k A'_k \sigma_a^{v_k} B^{v_k}(T_{j+\frac{1}{2}}^*), \quad (6.4)$$

at the approximate temperature

$$T_{j+\frac{1}{2}}^* = \frac{1}{2}(T_{j+\frac{1}{2}}^{n+1} + T_{j+\frac{1}{2}}^n).$$

The temperatures can then be determined by the energy balance equation (5.1c):

$$\rho \frac{(c_v T)_{j+\frac{1}{2}}^{n+1} - (c_v T)_{j+\frac{1}{2}}^n}{c \Delta t} = \sum_k A'_k \sigma_a^{v_k} \frac{1}{2} [E_{j+\frac{1}{2}}^{n+1}(v_k) + E_{j+\frac{1}{2}}^n(v_k)] - \bar{\sigma}_p(T_{j+\frac{1}{2}}^*) a \left[ \frac{1}{2}(T_{j+\frac{1}{2}}^{n+1} + T_{j+\frac{1}{2}}^n) \right]^4. \quad (6.5)$$

The temperature equation (6.5) is iterated to convergence using the Newton-Raphson Method [5], while holding the Planck mean constant at the approximate temperature  $T^*$ . The procedure is then repeated from (6.3) using the improved temperatures until the successive values converge to one part in  $10^4$ , usually within 2 or 3 iterations.

(d) *Calculation of zone-centered intensities*

Knowledge of the temperatures and zone boundary intensities permits the calculation of zone-centered intensities from the following difference form of (4.6):

$$\frac{I_{j+\frac{1}{2}}^{n+1} - I_{j+\frac{1}{2}}^n}{c \Delta t} + \mu_l \frac{I_{j+\frac{1}{2}}^{n+1} + I_{j+\frac{1}{2}}^n - I_j^{n+1} - I_j^n}{2(r_{j+1} - r_j)} + (\sigma_a^{v_k} + \sigma_s) \frac{1}{2}(I_{j+\frac{1}{2}}^{n+1} + I_{j+\frac{1}{2}}^n) = \sigma_a^{v_k} B^{v_k}(T_{j+\frac{1}{2}}^{n+\frac{1}{2}}) + \sigma_s S_{j+\frac{1}{2}}^{n+\frac{1}{2}}, \quad (6.6)$$

where

$$T_{j+\frac{1}{2}}^{n+\frac{1}{2}} = \frac{1}{2}(T_{j+\frac{1}{2}}^{n+1} + T_{j+\frac{1}{2}}^n),$$

and the scattering term is evaluated in terms of predicted intensities,

$$S_{j+\frac{1}{2}}^{n+\frac{1}{2}} = \sum_l \frac{1}{2} [I_{j+\frac{1}{2}}^{n+\frac{1}{2}}(l, k) + I_{j+\frac{1}{2}}^n(l, k)] \times A_l K(\mu_l, \mu_l).$$

With the intensities obtained from (6.6), the energy densities are given by the quadrature formula

$$E_{j+\frac{1}{2}}^{n+\frac{1}{2}}(v_k) = \frac{2\pi}{c} \sum_l A_l I_{j+\frac{1}{2}}^{n+\frac{1}{2}}(l, k). \quad (6.7)$$

These energy densities obey the difference form of (5.5a) by virtue of (4.7), and are therefore consistent with (6.3) which assures the conservation of energy.

The whole process can be repeated from (6.1), but it is usually more economical to reduce the time step  $\Delta t$ , if the calculation is not sufficiently accurate. The stability condition for the method has been determined experimentally to be

$$c \Delta t \leq \frac{1}{2} \Delta r.$$

The numerical procedure is illustrated for a number of sample calculations in section 7.

## 7. SAMPLE CALCULATIONS

The accuracy of the method is investigated in the solution of the following radiative heating problem. A semi-infinite slab of uniform density and specific heat is exposed to an external black-body radiation field at temperature  $T_0$ . The radiation and material energy densities are initially zero in the slab. The distributions of temperature and radiant energy are determined as a function of time.

Constant cross sections are considered first in order to illustrate the method for very long and



very short mean free path and to check the procedure for handling the scattering integral. A frequency-dependent problem is then solved, and the results are compared with those of the Monte Carlo method.

The calculations were coded in FORTRAN and performed on an IBM-7094. A typical execution of the discrete ordinate method requires 0.15 second per time step per frequency group. In all the calculations presented here, four Gaussian divisions of the angular interval were used,

$$\mu_l = \pm \frac{1}{2}(1 \pm 1/\sqrt{3}),$$

with a specific heat given by  $\rho c_v = 0.5917 a T_0^3$ .

(a) Constant cross sections

Temperatures calculated by the discrete ordinate method are shown in Fig. 2 for the case of

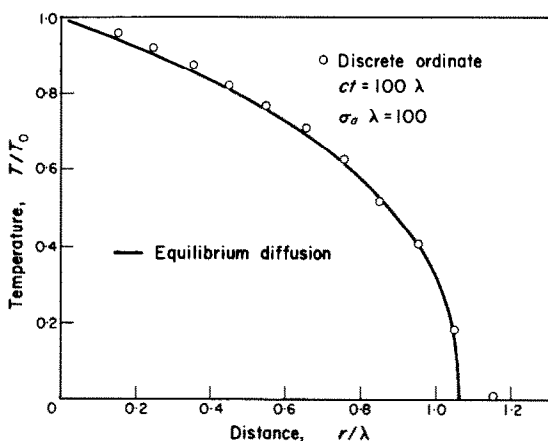


FIG. 2. Comparison of discrete ordinate and equilibrium diffusion calculations for large absorption cross section and no scattering. The discrete ordinate calculation was performed with  $c \Delta t = 0.05 \lambda$ ,  $\Delta r = 0.1 \lambda$ .

a mean free path small compared to the distance scale  $\lambda$ . These temperatures agree well with the similarity solution of the equilibrium diffusion equation given by Barfield *et al.* [17]. In Fig. 3 the discrete ordinate temperatures are compared with those obtained by the Monte Carlo calculation [4] for a mean free path large

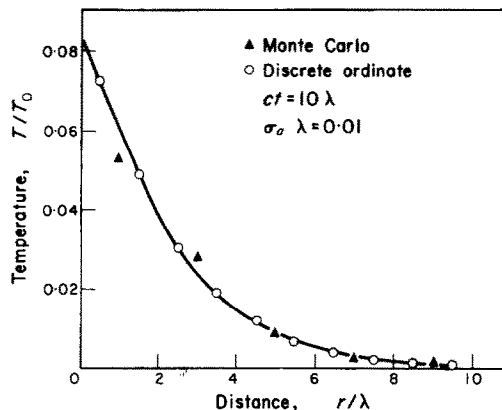


FIG. 3. Comparison of discrete ordinate and Monte Carlo calculations for small absorption cross section and no scattering. The discrete ordinate calculation was performed with  $c \Delta t = 0.5 \lambda$ ,  $\Delta r = 1.0 \lambda$ , and the 4000 particle Monte Carlo calculation with  $c \Delta t = 1.0 \lambda$ ,  $\Delta r = 1.0 \lambda$ .

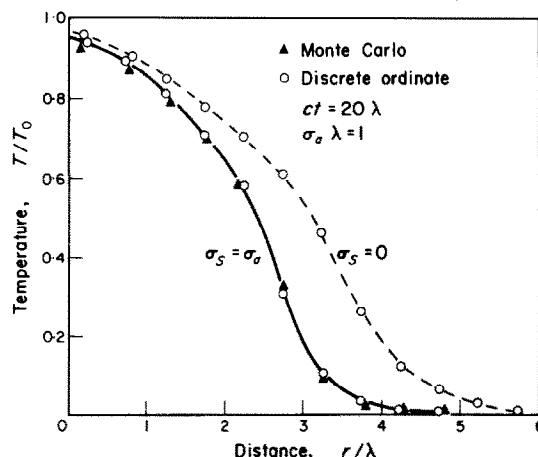


FIG. 4. The effect of Thompson scattering on energy penetration for constant cross sections. The discrete ordinate calculation was performed with  $c \Delta t = 0.25 \lambda$ ,  $\Delta r = 0.5 \lambda$ , and the 4000 particle Monte Carlo calculation with  $c \Delta t = 0.5 \lambda$  and  $\Delta r = 0.5 \lambda$ .

compared to the scale parameter  $\lambda$ . It is clear from these results that the difference method performs well in both cases.

In Fig. 4 the difference method is compared with Monte Carlo in a scattering problem. In the method presented in section 6, the scattering integral is evaluated in terms of extrapolated

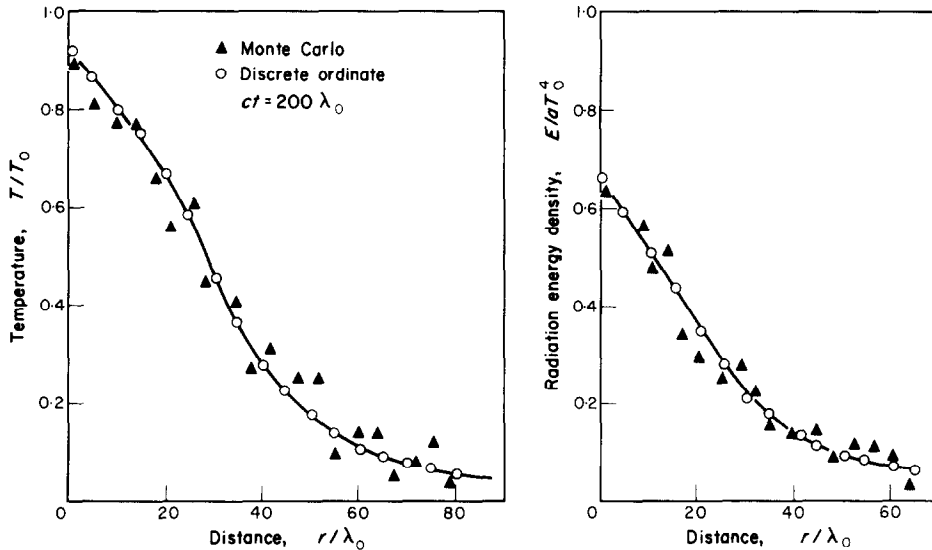


FIG. 5. Comparison of discrete ordinate and Monte Carlo methods for the frequency-dependent cross section  $\sigma_a = \sigma_0(h\nu/kT_0)^{-3}[1 - \exp(-h\nu/kT)]$  and no scattering. The discrete ordinate method was performed with  $c \Delta t = 0.5 \lambda_0$ ,  $\Delta r = 2.0 \lambda_0$ , and frequency differences  $\Delta(h\nu) = 0.5 kT_0$  with  $k_{\max} = 20$ . The 4000 particle Monte Carlo calculation was performed with  $c \Delta t = 1.0 \lambda_0$ ,  $\Delta r = 2.0 \lambda_0$ .

intensities. Since the predicted and corrected intensities do not generally agree, energy will not be strictly conserved. However, in Fig. 4 the method shows good agreement with the Monte Carlo calculation and gives overall energy conservation to within 0.01 per cent.

#### (b) Frequency-dependent cross sections

Figure 5 shows the results of a radiative heating calculation using the frequency-dependent cross section discussed in section 3. The distributions of temperature and frequency-integrated energy density are given for both the discrete ordinate and Monte Carlo calculations. The agreement is good, despite the statistical fluctuations of the Monte Carlo results. The difference calculation averaged 3 sec per cycle on the IBM-7094. The Monte Carlo calculation averaged 8 sec per cycle but used a time step double that of the difference method.

### 8. CONCLUSION

The results of the preceding section have shown that the finite difference method is generally superior to the Monte Carlo for the

simple problems considered here. The difference method requires less computing time and is free of statistical error. However, there are several areas in radiative transfer in which Monte Carlo techniques are superior. One such area involves the treatment of complicated geometries. Another is the nonconservative (Compton) scattering of radiation by hot electrons: a problem that occurs when the transport material is almost completely ionized.

It is apparent that each method has its own special advantages. Also, it frequently happens in numerical computation that one has little idea of the accuracy of his calculations. Under these conditions it is convenient to have two basically different methods with which to check the results.

Two aspects of the numerical computation that have not been considered in this paper are discontinuities in the angular distribution and spherical geometry. Both of these problems merely add to the complexity of the calculation and require no major alterations in the procedure.

A more important omission is the treatment

of cross sections with a complex structure of lines and absorption edges. This problem increases in difficulty as more detail in the frequency spectrum is required. Cross sections with edges and a few of the most prominent absorption lines are not too difficult to handle. Several calculations of this kind have been done with the discrete ordinate method and will be described in a forthcoming publication.

## REFERENCES

1. S. PAI, *Radiation Gas Dynamics*. Springer-Verlag, Berlin (1966).
2. R. PEARCE and A. MITCHELL, On finite difference methods of solution of the transport equation, *Math. Comput.* **16**, 155 (1962).
3. B. WENDROFF, The structure of certain finite difference schemes, *SIAM Rev.* **3**, 237 (1961).
4. P. CAMPBELL, Monte Carlo method for radiative transfer, *Int. J. Heat Mass Transfer* **10**, 519 (1967).
5. A. RALSTON and H. WILF, Editors, *Mathematical Methods for Digital Computers*, Part IV. John Wiley, New York (1960).
6. R. RICHTMYER, *Difference Methods for Initial-Value Problems*. Interscience, New York (1957).
7. H. MAYER, Methods of opacity calculations. *Los Alamos Scientific Laboratory Rep. No. AECD-1870* (1948).†
8. S. CHANDRASEKHAR, *Radiative Transfer*, p. 366. Dover Publications, New York (1960).
9. M. KROOK, On the solution of equations of transfer, *Astrophys. J.* **122**, 488 (1955).
10. C. KITTEL, *Elementary Statistical Physics*, p. 118. John Wiley, New York (1958).
11. W. MILNE, *Numerical Calculus*, Article 24. Princeton University Press, Princeton, N.J. (1949).
12. R. RICHTMYER, *Ibid.*, p. 93.
13. R. RICHTMYER, *Ibid.*, p. 169.
14. R. DE BAR, Private communication (1965).
15. G. SPILLMAN, Formulation of the Eddington factor for use in one-dimensional nonequilibrium diffusion calculations, *Los Alamos Scientific Laboratory Memorandum* (1968).
16. P. CAMPBELL and R. NELSON, Numerical methods for calculating nonlinear radiation transport. *Lawrence Radiation Laboratory Rep. No. UCRL-7838* (1964).†
17. W. BARFIELD, R. VON HOLDT and F. ZACHARIASEN, A comparison of diffusion theory and transport theory results for the penetration of radiation into plane semi-infinite slabs. *Los Alamos Scientific Laboratory Rep. No. AECD-3653* (1954).†

† These documents can be obtained from the Clearinghouse for Federal Scientific and Technical Information, National Bureau of Standards, U.S. Department of Commerce, Springfield, Va.

**Résumé**—On présente une méthode de solution numérique des problèmes non-linéaires du transport par rayonnement dépendant de la fréquence et à symétrie unidimensionnelle. La caractéristique principale de la méthode est la précision du schéma de différences finies dans les cas limites des grandes et des petites sections droites. La méthode est illustrée par de nombreux calculs d'exemples.

**Zusammenfassung**—Es wird eine Methode zur Lösung nichtlinearer, frequenzabhängiger Strahlungsprobleme mit eindimensionaler Symmetrie angegeben. Das Hauptmerkmal der Methode ist die Genauigkeit des endlichen Differenzschemas in den Grenzen von grossen und kleinen Querschnitten. Die Methode wird durch eine Reihe von Rechenbeispielen veranschaulicht.

**Аннотация**—Представлен метод численного решения нелинейных, зависящих от частоты, задач лучистого переноса с одномерной симметрией. Основной особенностью метода является точность схемы конечных разностей в пределах больших и малых поперечных сечений. Метод иллюстрируется на ряде примеров.